Available online at www.elixirpublishers.com (Elixir International Journal)

Chemical Physics

Elixir Chem. Phys. 94 (2016) 39982-39992

ISSN: 2229-712X

Quantum chemical investigations and FTIR, FT-Raman, NMR, FMO, NBO, MESP of 1,2,4-triazine-3,5(2H,4H)-dione

P. Dinesh

Department of Physics, Salem Sowdeswari College, Salem 636 010, India.

ARTICLE INFO

Article history:

Received: 14 March 2016;

Received in revised form:

29 April 2016;

Accepted: 2 May 2016;

Keywords

1,2,4-triazine-3,

5(2H,4H)-dione,

FT-IR,

FT-Raman,

HOMO-LUMO,

MESP,

NBO.

ABSTRACT

The experimental and theoretical study on the structure and vibrations of 1,2,4-triazine-3,5(2H,4H)-dione have been carried out by *ab initio* HF and DFT/B3LYP method with 6-311++G(d,p) basis set. The FT-IR and FT-Raman spectra of the title compound have been recorded. The molecular structure, vibrational wavenumbers, infrared intensities and Raman activities were calculated. The force constants obtained from this study have been utilized in the normal coordinate analysis (NCA). The temperature dependence of thermodynamic properties has been analyzed. Molecular electrostatic potential (MESP), total electron density distribution and frontier molecular orbital's (FMO) were constructed at B3LYP/6-311++G(d,p) level to understand the electronic properties. The atomic charges, electronic exchange interaction and charge delocalization of the molecule have been performed by natural bond orbital (NBO) analysis.

1.Introduction

Triazine and their derivatives have been proved to be effective anti-cancer, anti-HIV and anti-fungal activities [1]. Derivatives of 1,2,4-triazine are known to exhibit fungicidal, insecticidal, bactericidal, herbicidal, antimicrobial and antimalarial agents[2-7]. The compound 1,2,4-triazine-3,5(2H,4H)-diones (TD) and their thiones (6-azauracil derivatives) possess [8-10] biological activity as cytotoxic, antiviral, enzyme inhibiting, immunosuppressive, antiphlogestic and bacteriostatic agents [11,12]. Compounds containing thiophene are well known to exhibit various biological activities such as anti-HIV PR inhibitors [13], anti-breast cancer (MCF-7) [14], anti-inflammatory [15-17], anti-protozoal [18], anti-tumor [19], anti-tubercular with anti-mycobacterial activity [20]. On the otherhand, the 1,2,4-triazine moiety has also attracted the attention of chemists because many 1,2,4-triazines are biologically active [21-26] and are used in medicine [27-31 as well as in agriculture [32-35]. It is well established in plant protection fungicides include epoxiconazole, triadimenol, propiconazole, metconazole, cyproconazole, tebuconazole, flusilazole and paclobutrazol [36- 38].

Vibrational spectroscopy (IR and Raman) techniques are widely used to study structural and dynamical aspects of molecular systems. With the recent advances in computational methods and common access to large-scale powerful computers and currently available theoretical methods allow a quite precise prediction of experimental IR and Raman spectra of rigid, medium-size molecules. For most of such systems, the theoretically calculated frequencies and intensities of the IR and Raman bands are close to experimental value. Hence, one may expect that the normal modes, obtained using the theoretically predicted force field, should also reflect well the forms of variations in a real molecule. Normal mode analysis is commonly employed in the interpretation of the vibrational spectra [39]. Usually, the calculated normal modes are described in terms of potential energy distribution [PED]. In the PED analysis, the energy of a normal vibration is interpreted as a sum of contributions from particular internal (or symmetry) coordinates. Now-a-days evolution of density functional theory (DFT) [40] method has been accepted as a popular Post-HF approach for computation of molecular structure, vibrational frequencies and other molecular properties.

To the best of our knowledge, there is no *ab initio* HF and DFT based Becke3–Lee–Yang–Parr (B3LYP) functional with standard 6-311++G(d,p) basis set of TD has been reported so far. It has been felt that a through knowledge of different normal modes of vibrations could be of much help to understand such properties of these compounds. As vibrational spectroscopy is believed to be an effective experimental technique for such understanding, Raman and IR spectra of TD have been critically examined and special attention has also been paid to explain all the remarkable qualitative and quantitative differences in these spectra.

2. Experimental details

The fine polycrystalline sample of 1,2, 4-triazine-3,5(2H,4H)-dione (TD) was purchased from Alfa Aesar chemical company, UK with a stated purity of 98% and it was used as such without further purification. The room temperature Fourier transform infrared spectra of the title compound was measured in the region 4000 – 400 cm^{-1} at a resolution of ±1 cm^{-1} using a JASCO FT/IR–6300 spectrometer. KBr pellets were used in the spectral measurements. Boxcar apodization was used for 250 averaged interferograms collector for both the sample and background.

The FT-Raman spectrum of the title compound was recorded on a BRUKER IFS model interferometer equipped with an FRA-106 FT-Raman accessory in the 3500 – 50 cm^{-1} Stokes region using the 1064nm line of Nd:YAG laser for

Tele: +91 94881 12792

E-mail address: pgdineshp6@gmail.com

excitation, operating at 150mW power. The reported wave numbers are believed to be accurate within ± 1 cm^{-1}.

3. Computational details

Ab initio and DFT computations of TD were performed by using GAUSSIAN 09W program package [41] with 6-311++G(d,p) basis set to derive the complete geometry optimization. Further, the energy calculation, vibrational frequencies, IR intensities and Raman activities were carried out for TD with the GAUSSIAN 09W software package using Hartree-Fock (HF) and DFT/B3LYP functional combined with the standard 6-311++G(d,p) basis set. Initial geometry generated from the standard geometrical parameters was minimized without any constraint on the potential energy surface at Hartree-Fock level adopting the standard 6-311++G(d,p) basis set. This geometry was then re-optimized again at DFT level employing the B3LYP method [42-44] using the correlation function of Lee et al., [45] implemented with the same basis set for better description of the bonding properties. All the parameters were allowed to relax and all the calculations converged to an optimized geometry which corresponds to a true minimum and the absence of the imaginary frequencies are ensured. The Cartesian representation of the theoretical force constants have been computed at the fully optimized geometry. In order to have better agreement with the experimental data, the multiple scaling of the force constants were performed according to SQM procedure [43,44] using relative scaling in the natural internal coordinate representation [46,47]. Transformations of the force field, and the subsequent normal coordinate analysis (NCA) including the least square refinement of the scaling factors, calculation of the potential energy distribution (PED) and the prediction of IR intensities and Raman activities were done on a PC with the MOLVIB Program (Version V7.0-G77) written by Sundius [48-50]. Further, the frontier molecular orbital (HOMO-LUMO) analysis, NBO/NLMO analysis, MESP analysis have been made using DFT/B3LYP method with 6-311++G(d,p) basis set.

A better agreement between the computed and experimental frequencies can be obtained by using different scale factors for different types of fundamental vibrations. To determine the scale factors, the procedures used previously [51–57] has been followed that minimises the residual separating experimental and theoretically predicted vibrational frequencies. The optimum scale factors for vibrational frequencies were determined by minimising the residual

$$\Delta = \sum_{i}^{N} (\lambda\omega_i^{theor} - \nu_i^{Expt})^2$$

Where ω_i^{Theor} and ν_i^{Expt} are the i^{th} theoretical harmonic frequency and i^{th} experimental fundamental frequency (in cm^{-1}), respectively and N is the number of fundamental modes which leads to

$$RMS = \sqrt{\frac{\Delta}{N}}$$

3.1. Prediction of Raman intensities

The Raman scattering activities (S_i) calculated by Gaussian 09W program were suitably converted to relative Raman intensities (I_i) using the following relationship derived from the basic theory of Raman scattering [58-60].

$$I_i = \frac{f(\nu_0 - \nu_i)^4 S_i}{\nu_i [1 - \exp(-hc\nu_i / kT)]}$$

Where, v_o is the exciting frequency (cm^{-1}), v_i is the vibrational wavenumber of the i^{th} normal mode, *h*, *c* and *k* are universal constants, and *f* is the suitably chosen common scaling factor for all the peak intensities.

4. Results and discussion

4.1 Molecular geometry

The molecular structure of TD is shown in Fig 1. A complete geometrical optimization was performed within the C_s point group symmetry. Molecular symmetry can be used to predict many molecular properties, such as its dipole moment and its allowed spectroscopic transitions. The calculated optimized geometrical parameters obtained in this study for TD are presented in Table 1.

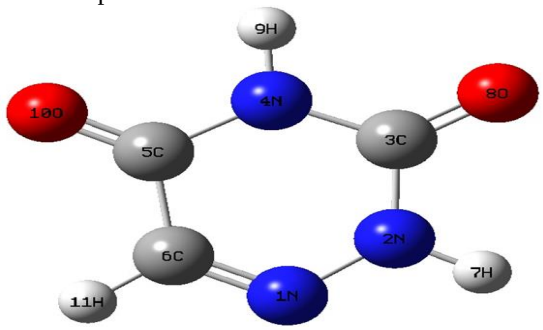

Fig 1.Molecular structure of 1,2,4-triazine-3,5(2H,4H)-dione along with numbering of atoms.

Table 1.Optimized geometrical parameters of 1,2,4-triazine-3,5(2H,4H)-dione obtained by HF/6-311++G(d,p) and B3LYP/6-311++G(d,p) density functional calculations.

Bond Length	Value (Å)		Bond Angle	Value(°)			Value(°)	
	HF/ 6-311++G(d,p)	B3LYP/ 6-311++G(d,p)		HF/ 6-311++G(d,p)	B3LYP/ 6-311++G(d,p)	Dihedral Angle	HF/ 6-311++G(d,p)	B3LYP/ 6-311++G(d,p)
N1-N2	1.34	1.35	N2-N1-C6	119	118.07	C6-N1-N2-H7	180	-180.0
N1-C6	1.26	1.29	N1-N2-C3	126.35	127.08	N2-N1-C6-H11	180	180.0
N2-C3	1.37	1.39	N1-N2-H7	115.9	115.84	N1-N2-C3-O8	180	-180.0
N2-H7	0.99	1.01	C3-N2-H7	117.75	117.08	H7-N2-C3-N4	-180	180.0
C3-N4	1.37	1.39	N2-C3-N4	113.3	112.29	N2-C3-N4-H9	180	180.0
C3-O8	1.19	1.21	N2-C3-O8	123.2	123.18	O8-C3-N4-C5	-180	180.0
N4-C5	1.38	1.40	N4-C3-O8	123.5	124.53	C3-N4-C5-O10	180	180.0
N4-H9	1	1.01	C3-N4-C5	125.45	126.10	H9-N4-C5-C6	180	180.0
C5-C6	1.48	1.48	C3-N4-H9	116.46	116.31	N4-C5-C6-H11	-180	-180.0
C5-O10	1.18	1.21	C5-N4-H9	118.09	117.60	O10-C5-C6-N1	-180	180.0
C6-H11	1.07	1.08	N4-C5-C6	112.89	112.54			
			N4-C5-O10	123.08	122.41			
			C6-C5-O10	124.03	125.04			
			N1-C6-C5	123	123.92			
			N1-C6-H11	118.85	117.85			
			C5-C6-H11	118.15	118.23			

For numbering of atoms refer Fig.1

Detailed description of vibrational modes can be given by means of normal coordinate analysis (NCA). For this purpose, the full set of 38 standard internal coordinates (containing 11 redundancies) for TD is presented in Table 2. From these, a non-redundant set of local symmetry coordinates were constructed by suitable linear combination of internal coordinates following the recommendations of Pulay and Fogarasi [61,62], which are presented in Table 3. The theoretically calculated DFT force fields were transformed to this latter set of vibrational coordinates and used in all subsequent calculations.

Table 2.Definition of internal coordinates of 1,2,4-triazine-3,5(2H,4H)-dione.

No(i)	Symbol	Type	Definition[a]
Stretching			
1-3	r_i	C-N	C_3-N_2, C_3-N_4, C_5-N_4, C_6-N_1
5-6	T_i	C-O	C_3-O_8, C_5-O_{10}
7-8	R_i	N-H	N_2-H_7, N_4-H_9
9	Q_i	C-H	C_6-H_{11}
10	P_i	N-N	N_1-N_2
11	S_i	C-C	C_5-C_6
Bending			
12-17	β_i	Ring	N_1-N_2-C_3, N_2-C_3-N_4, C3-N_4-C_5, N_4-C_5-C_6, C_5-C_6-N_1, C_6-N_1-N_2
18-20	α_i	N-C-O	N_2-C_3-O_8, N_4-C_3-O_8, N_4-C_5-O_{10}
21	α_i	C-C-O	C_6-C_5-O_{10}
22	δ_i	N-N-H	N_1-N_2-H_7
23-25	δ_i	C-N-H	C_3-N_2-H_7, C_3-N_4-H_9, C_5-N_4-H_9
26	θ_i	C-C-H	C_5-C_6-N_1
27	θ_i	N-C-H	N_1-C_6-H_{11}
Out of plane Bending			
28-29	ω_i	N-H	H_7-N_2-N_1-C_3, H9-N4-C_3-C_5
30-31	ω_i	C-O	O_8-C_3-N_2-N_4, O_{10}-C_5-N_4-C_6
32	ω_i	C-H	H_{11}-C_6-N_1-C_5
Torsion			
33-38	τ_i	τ Ring	N_1-N_2-C_3-N_4, N_2-C_3-N_4-C_5, C_3-N_4-C_5-C_6, N_4-C_5-C_6-N_1, C_5-C_6-N_1-N_2, C_6-N_1-N_2-C_3

[a]For numbering of atoms refer Fig. 1

Table 3. Definition of local symmetry coordinates of 1,2,4-triazine-3,5(2H,4H)-dione..

No(i)	Symbol[a]	Definition [b]
1-4	CN	r_1, r_2, r_3, r_4
5-6	CO	T_5, T_6
7-8	NH	R_7, R_8
9	CH	Q_9
10	NN	P_{10}
11	CC	S_{11}
12	Rtrigd	$(\beta_{12}- \beta_{13}+ \beta_{14}- \beta_{15}+ \beta_{16}+ \beta_{17}) / \sqrt{6}$
13	Rsymd	$(\beta_{12}- \beta_{13}+2\ \beta_{14}- \beta_{18}- \beta_{19}+ 2\ \beta_{20}) / \sqrt{12}$
14	Rasymd	$(\beta_{12}- \beta_{13}+ \beta_{15}- \beta_{16}) / \sqrt{2}$
15-16	bCO	$(\alpha_{18}- \alpha_{19}) /\sqrt{2}$, $(\alpha_{20}- \alpha_{21}) / \sqrt{2}$
17-18	bNH	$(\alpha_{22}- \alpha_{23}) / \sqrt{2}$, $(\alpha_{24}- \alpha_{25}) / \sqrt{2}$
19	bCH	$(\theta_{26}- \theta_{27}) / \sqrt{2}$
20-21	ωNH	ω_{28}, ω_{29}
22-23	ωCO	ω_{30}, ω_{31}
24	ωCH	ω_{32}
25	τ Rtrigd	$(\tau_{33}- \tau_{34}+ \tau_{35}- \tau_{36}+ \tau_{37}- \tau_{38}) / \sqrt{6}$
26	τ Rsymd	$(\tau_{33}- \tau_{35}+ \tau_{36}- \tau_{37}) / \sqrt{12}$
27	τ Rasymd	$(-\tau_{33}- \tau_{34}- \tau_{35}- \tau_{36}+ \tau_{37}- \tau_{38}) / \sqrt{2}$

[a] These symbols are used for description of the normal modes by PED in Tables 5

[b] The internal coordinates used here are defined in Table 2

4.2 Thermodynamic analysis.

The energies and thermodynamic parameters of TD employing *ab initio* HF and DFT/B3LYP method with 6-311++G (d, p) basis sets are presented in Table 4. The frequency calculation computes the zero point vibrational energies, thermal correction to internal energy, enthalpy, Gibbs free energy and entropy as well as heat capacity for a molecular system. The thermodynamic data gives the detailed information for further study on the title compound, when there may be used as a reactant to take part in new reactions.

Table 4.The thermodynamic parameters of calculated 1,2,4-triazine-3,5(2H,4H)-dione HF/ 6-311G++ (d,p)and / B3LYP/6-311G++ (d,p)methods.

Parameter	HF/ -11++G(d,p)	B3LYP/ 6-11++G(d,p)
SCF energy (Hartrees)	-428.54613	-430.95872
Zero-point vibrational Energy (kJ/mol)	50.81957	46.73651
Rotational constants (GHz)	4.03970	3.95050
	2.11483	2.04904
	1.38813	1.34922
Thermal energy (kJ/mol)		
Total	54.468	50.584
Translational	0.889	0.889
Rotational	0.889	0.889
Vibrational	52.691	48.807
Molar capacity at constant volume ($calmol^{-1}Kelvin^{-1}$)		
Total	21.059	22.638
Translational	2.981	2.981
Rotational	2.981	2.981
Vibrational	15.097	16.677
Entropy ($calmol^{-1}Kelvin^{-1}$)		
Total	77.979	79.081
Translational	40.083	40.083
Rotational	27.696	27.778
Vibrational	10.200	11.220
Dipole moment (Debye)		
μ_x	0.1978	0.5845
μ_y	1.8962	1.6829
μ_z	0.0000	0.0000
μ_{total}	1.9065	1.7815

5. Vibrational analysis

The title molecule consists of 11 atoms. Under C_s symmetry, 27 fundamentals of TD are distributed amongst the symmetry species as

$\Gamma_{Vib} = 19A' + 8A''$

All the vibrations are active in both IR and Raman. The combined FT-IR and FT-Raman spectra of the compound under investigation are shown in Figs. 2 and 3, respectively. The observed and calculated frequencies using *ab initio* HF

and DFT/B3LYB method with 6-311++G(d,p) basis sets along with their relative intensities, detailed vibrational assignments and potential energy distribution (PED) of TD were summarised in Table 5.

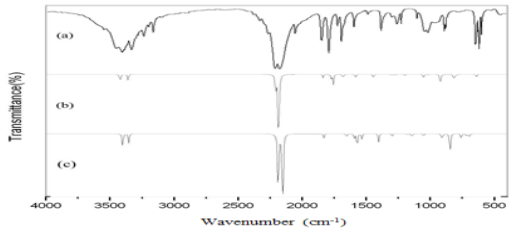

Fig 2.Comparison of observed and calculated IR spectra of 1,2,4-triazine-3,5(2H,4H)-dione (a) observed; (b) calculated with HF/6-311++G(d,p); (c) Calculated with B3LYP/6-311++G(d,p).

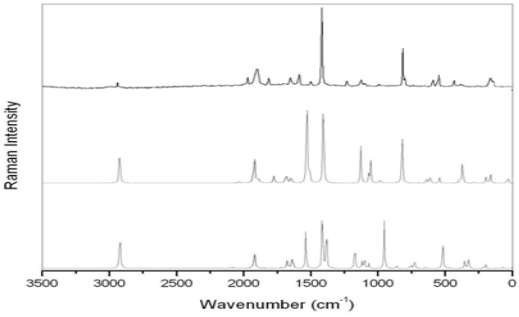

Fig3.Comparison of observed and calculated Raman spectra of 1,2,4-triazine-3,5(2H,4H)-dione (a) observed; (b) calculated with HF/6-311++G(d,p) (c) Calculated with B3LYP/6-311++G(d,p).

5.1 C-H Vibration

Usually the bands in the range 3100-3000 cm^{-1} are assigned to C-H stretching vibrations of aromatic compounds, which is the characteristic region for the ready identification of C-H stretching vibrations [63]. In this region, the bands are not affected appreciably by the nature of the substituent, the C-H stretching modes usually appear with strong Raman intensity and are highly polarized. Fundamental mode observed at 3125 and 3096 cm^{-1} in FTIR and FT Raman, respectively, are assigned to the C-H stretching vibration of TD. The C-H in-plane bending vibrations are observed in the region 1350-950 cm^{-1}. The frequency of the C-H out-of-plane bending modes depends mainly on the number of the adjacent hydrogen atoms on the ring and not very much affected by the nature of substituents. The C-H out-of-plane bending modes usually medium to strong intensity arises in the region 950-600 cm^{-1} [64-66]. In this study, the C-H in-plane bending vibration is assigned to 1023 cm^{-1} in FTIR and 1021 cm^{-1} in FT Raman. The CH out-of-plane bending vibration is observed 749 cm^{-1} in FTIR and 746 cm^{-1} in FT-Raman. Above mentioned CH in-plane and out-of-plane bending mode of the title compound is well agreed with reported data [67-69].

5.2 N-H Vibration

It has been observed that the presence of N-H atomic group in various molecule may be correlated with a constant occurrence of absorption bands whose positions are slightly altered from one compound to another. This is because the atomic group vibrates independently of the other groups in the molecule and has its own frequency. Normally in all the heterocyclic compounds, the N-H stretching vibration occurs in the region 3500-3000 cm^{-1} [70, 71]. The position of absorption in this region depends upon the degree of hydrogen bonding, and hence upon the physical state of the sample.

Table 5. The observed FTIR, FT-Raman and calculated (Unscaled and Scaled) frequencies (cm^{-1}) and probable assignments (characterized by PED) of 1,2,4-triazine-3,5(2H,4H)dione using HF/6-311++G(d,p)and B3LYP/6-311++G(d,p)calculations.

S.No	Observed frequencies (cm^{-1})		HF /6-311++G(d,p)		B3LYP / 6-311 ++G(d,p)						Assignments (PED)
	FT-IR	FT-Raman	UnScaled	Scaled	IR Intensity	Raman Activity	UnScaled	Scaled	IR Intensity	Raman Activity	
1	3361	-	3892	3384	4.75	0.039	3630	3364	3.34	0.008	NH(100)
2	3217	-	3830	3231	0.50	0.248	3583	3221	0.37	0.427	NH(100)
3	3125	3096	3380	3139	35.51	1.369	3212	3129	24.10	1.785	CH(98)
4	1798	1790	1995	1818	8.47	1.390	1813	1803	4.93	0.698	C=O(96)
5	1750	-	1972	1777	12.36	4.697	1779	1756	7.30	5.681	C=O(94)
6	1687	1669	1861	1699	31.29	0.274	1641	1679	26.09	0.409	CC(85), CN(10)
7	1599	1598	1623	1609	56.47	0.133	1468	1602	14.31	4.152	NN(82), NH(13)
8	1451	1454	1560	1468	16.85	2.358	1410	1456	41.58	0.276	CN(80), bNH(15)
9	-	1445	1544	1456	178.68	0.534	1388	1450	144.68	0.504	CN(81), CO(17)
10	1408	1408	1468	1419	13.66	10.651	1351	1412	10.86	16.857	CN(80), bCH(15)
11	1359	-	1370	1368	1.78	2.171	1224	1361	27.74	0.361	bNH (79), NN(20)
12	1336	-	1230	1349	60.92	0.226	1123	1340	9.74	0.522	CN(77), bCO(19)
13	1267	1265	1090	1277	23.65	2.869	1044	1271	20.56	0.893	bNH(76),CN(21)
14	1023	1021	1060	1039	26.43	4.087	972	1028	29.85	5.838	bCH (69), Raymd(19)
15	998	-	986	1013	16.58	2.194	883	1005	11.35	2.706	Rtrigd(64),CH(17)
16	865	-	837	872	52.68	0.368	750	869	23.57	1.921	bCO(65), CN(21)
17	855	-	821	810	54.02	26.167	742	853	60.22	25.940	bCO(67), Rtrigd(23)
18	845	-	798	856	69.06	2.352	739	847	37.87	2.916	Rsymd(63), bNH(21)
19	753	753	707	767	149.17	11.096	682	759	114.64	7.789	Rasymd(60), CC(24)
20	749	746	608	754	60.96	4.395	597	747	35.45	4.507	ω CH(59), tRasym(21)
21	576	578	602	588	53.05	18.857	558	581	28.82	15.598	τRsymd(57), ω CO(26)
22	573	-	589	580	12.60	60.800	539	577	33.12	24.461	ω NH(53), τRtrig(19)
23	562	-	571	573	1424.73	8.570	525	568	691.66	48.077	τRtrig(55), ω CH(27)
24	-	444	435	568	311.86	64.143	406	559	555.54	29.173	ω NH(53), τRsymd(19)
25	-	397	424	557	0.03	84.607	384	542	0.22	99.682	ω CO(51), ω CH(23)
26	-	228	152	239	102.47	56.296	152	232	71.02	78.463	ω CO(52), ω CH(21)
27	-	150	144	158	134.74	80.743	138	153	111.37	102.101	τRasym(53)

Abbreviations:R- ring; b – bending; ω-out-of-plane bending; τ-torsion; trigd-trigonal deformation; symd-symmetric deformation; asymd – antisymmetric deformation; ν-stretching.

The spectral lines assigned to N-H stretching vibrations have shifted to higher region in the present system. It is clearly indicates that the stretching N-H bond upon protonation has shifted the frequency to a higher region. Another possible cause for the stretching may be due to the occurrence of N-H and C-H hydrogen bonds in the atomic sites of the ring compounds. Hence, in the present investigation, the N-H stretching vibrations have been observed at 3361 and 3217 cm^{-1} in IR, which are further supported by the PED contribution of almost 100%.

5.3 C=O Vibration

The C=O stretch lies in the spectral range 1860-1750 cm^{-1} and is very intense in the infrared and only moderately active in Raman. The interaction of carbonyl group with other groups present in the system did not produce such a drastic and characteristic changes in the frequency of C=O stretch as did by interaction of N-H stretch. The carbon-oxygen double bond is formed by $P_\pi - P_\pi$ between carbon and oxygen, the bonding electrons are not equally distributed between the two atoms. The lone pair of electrons are oxygen also determines the nature of the carbonyl group. The position of the C=O stretching vibration is very sensitive to various factors such as the physical state, electronic effects by substituents, ring strains [72]. Normally carbonyl group vibrations occur in the region 1850-1600 cm^{-1} [73]. In this study, the C=O stretching vibrations of TD are observed at 1798, 1750 cm^{-1} in FTIR and 1790 cm^{-1} in the FT-Raman. The in-plane and out-of-plane bending vibrations of C=O group have also been identified and presented in Table 5 for the title molecule.

5.4 C-N vibration

In aromatic compounds, the C-N stretching vibrations usually lies in the region 1400-1200 cm^{-1}. The identification of C-N stretching frequencies is a rather difficult task, since the mixing of vibrations is possible in this region [74,75]. In this study, the bands observed at 1451, 1408, 1359 cm^{-1} in FTIR and 1454, 1445, 1445, 1408 cm^{-1} in FT Raman spectrum have been assigned to C-N stretching vibration of TD. These assignments an also supported by the PED values.

6. HOMO–LUMO analysis

Many organic molecules containing conjugated π electrons are characterized as hyperpolarizabilities and are analysed by means of vibrational spectroscopy [76,77]. In most cases, even in the absence of inversion symmetry, the strongest bands in the Raman spectrum are weak in the IR spectrum and vice versa. But the intramolecular charge transfer from the donor to acceptor group through a single–double bond conjugated path can induce large variations of both the molecular dipole moment and the molecular polarizability, making IR and Raman activity at the same time. The experimental spectroscopic behaviour described above is well accounted, for by DFT calculations in π conjugated systems that predict exceptionally large Raman and infrared intensities for the same normal modes [76]. It is also observed in our title molecule, the bands in FT-IR spectrum have their counterparts in Raman shows that the relative intensities in IR and Raman spectra are comparable resulting from the electron cloud movement through π conjugated frame work electron donor to electron acceptor groups. The analysis of the wave function indicates that the electron absorption corresponds to the transition from the ground to the first excited state and is mainly described by one-electron excitation from the highest occupied molecular orbital (HOMO) to the lowest unoccupied molecular orbital (LUMO). The LUMO of π nature, (i.e. benzene ring) is delocalized over the whole C-C bond. Consequently the HOMO–LUMO transition implies an electron density transfer to almost all the atoms. The atomic orbital compositions of the frontier molecular orbital and few MOs are sketched in Fig 4. The energy gap reflects the chemical activity of the molecule. LUMO as an electron acceptor represents the ability to obtain an electron, HOMO represents the ability to donate the electron.

HOMO energy = -0.09388a.u

LUMO energy = -0.29271a.u

HOMO–LUMO energy gap ΔE = 0.38659a.u.

Moreover lower in the HOMO–LUMO energy gap explains the eventual charge transfer interactions taking place within the molecule.

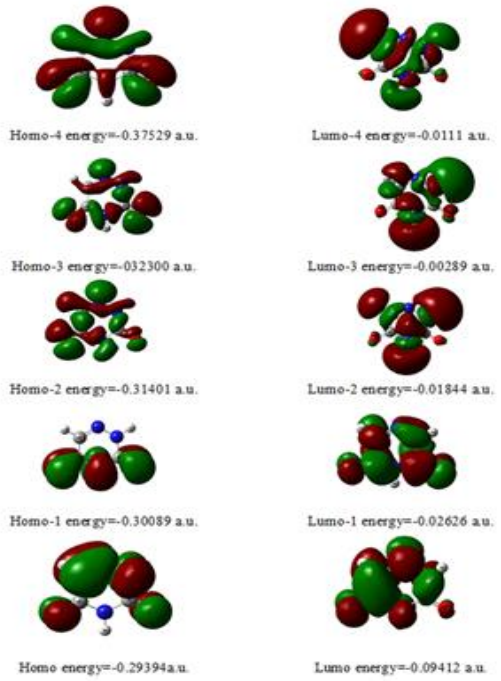

Fig 4.Surfaces of FMOs for1,2,4triazine3,5(2H,4H)-dione (orbital numbers are extracted from the output results of the B3LYP calculation).

7. Mulliken and Natural population analysis (NPA)

The charge distributions calculated by the Mulliken method for the equilibrium geometry of TD with DFT/6-311++G (d, p) are listed in Table 6. The charge distribution on the molecule has an important influence on the vibrational spectra. The corresponding Mulliken's plot is shown in Fig. 5. The atomic charges in the CH group are almost identical. The atomic charges obtained from 6-311++G (d, p) basis set shows that C5 atom is more acidic due to more positive charge whereas H7 and H9 are more negative (Table 6).

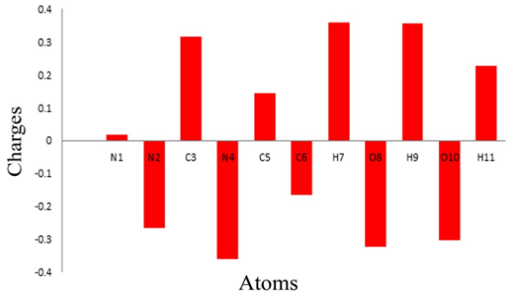

Fig 5. Plot of Mulliken charges of 1,2,4-triazine-3,5(2H,4H)-dione.

Since the charge distribution on the molecule has an important influence on the vibrational spectra, the net charge distribution of TD was calculated by the natural population analysis (NPA) method with B3LYP/6-311G++(d,p) basis sets and the charges are listed in Table 6. The corresponding NPA plot is shown in Fig. 6. The atomic charges of TD calculated by NPA analysis using B3LYP methods with 6-311++G(d,p) basis sets are presented in Table 6. Among the carbon atoms C3 and C5 have positive charge while C6 have negative charge.

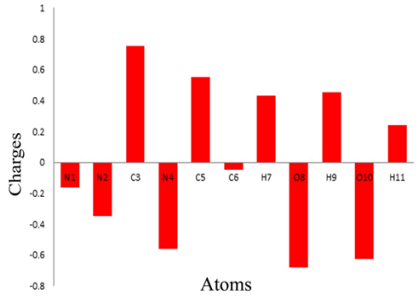

Fig 6. Plot of NPA charges of 1,2,4-triazine-3,5(2H,4H)-dione.

Table 6.The charge distribution calculated by Mulliken and Natural Population Analysis (NPA) methods for 1,2,4-triazine-3,5(2H,4H)-dione using B3LYP/6-311++G(d,p).

Atoms	Atomic charges	
	Mulliken	NPA
	B3LYP/ 6-311++G(d,p)	B3LYP/ 6-311++G(d,p)
N1	0.0190	-0.1629
N2	-0.2654	-0.3486
C3	0.3170	0.7515
N4	-0.3617	-0.5596
C5	0.1430	0.5493
C6	-0.1651	-0.0471
H7	0.3579	0.4307
O8	-0.3249	-0.6782
H9	0.3555	0.4531
O10	-0.3037	-0.6286
H11	0.2285	0.2403

Table 7.The atomic orbital occupancies of 1,2,4-triazine-3,5(2H,4H)-dione.

Atom no.	Atomic orbital	Type	Occupancy	Energy
N1	1S	Core	1.99948	-14.26325
	2S	Valence	1.35229	-0.58917
	2Px	Valence	1.07492	-0.21985
	2Py	Valence	1.61970	-0.29502
	2Pz	Valence	1.08945	-0.27194
N2	1S	Core	1.99923	-14.29742
	2S	Valence	1.20201	-0.60345
	2Px	Valence	1.28865	-0.33024
	2Py	Valence	1.27794	-0.34330
	2Pz	Valence	1.55500	-0.35440
C3	1S	Core	1.99934	-10.26135
	2S	Valence	0.76974	-0.22527
	2Px	Valence	0.80851	-0.11258
	2Py	Valence	0.80397	-0.08960
	2Pz	Valence	0.83176	-0.19773
N4	1S	Core	1.99910	-14.25393
	2S	Valence	1.24601	-0.61897
	2Px	Valence	1.31191	-0.34416
	2Py	Valence	1.43257	-0.35768
	2Pz	Valence	1.55593	-0.34416
C5	1S	Core	1.99903	-10.21558
	2S	Valence	0.83088	-0.21946
	2Px	Valence	0.79475	-0.09206
	2Py	Valence	0.95936	-0.11504
	2Pz	Valence	0.83359	-0.18107
C6	1S	Core	1.99909	-10.13968
	2S	Valence	0.95477	-0.24987
	2Px	Valence	1.02527	-0.11374
	2Py	Valence	1.05666	-0.13030
	2Pz	Valence	0.98442	-0.18812
H7	1S	Valence	0.56519	0.01666
O8	1S	Core	1.99990	-18.93526
	2S	Valence	1.82219	-0.92330
	2Px	Valence	1.49461	-0.26017
	2Py	Valence	1.75700	-0.26827
	2Pz	Valence	1.59656	-0.26019
H9	1S	Valence	0.54191	0.03598
O10	1S	Core	1.99990	-18.93415
	2S	Valence	1.81569	-0.92014
	2Px	Valence	1.47621	-0.25795
	2Py	Valence	1.81205	-0.26733
	2Pz	Valence	1.51677	-0.25572
	1S	Valence	0.75772	0.00317

The positive charge of C3 and C5 are due to the resonance nature of the C=O group. The very high positive charge on the carbon C3 is due to the partial polar nature of C=O group assignment of the hybridization of atomic lone pairs of the atoms involved in bond orbitals. Interaction between atomic orbitals can be interpreted using NBO theory. NBO analysis encompass a suite of algorithm's that enable fundamental bonding concepts to be extracted from Hartree-Fock, DFT and Post-HF computations. NBO analysis of molecule illustrate the deciphering of the molecular wave function in terms commonly understood by chemists: Lewis structures charge, bond order, bond type, hybridisation, resonance, donor-acceptor interactions, etc., NBO also gives the accurate natural Lawis structure picture of (θ) since it gives the maximum percentage of electron density using mathematical formulation of orbitals. NBO analysis originated as a technique for studying hybridisation and covalency effects in polyatomic wave functions, based on local block Eigen vector of the one-particle density matrix.

The NBO analysis has been performed for the title molecule using NBO 3.1 program as implemented in the GAUSSIAN 09W package at the DFT/B3LYP/6-311++G(d,p) level in order to elucidate atomic charges, atomic orbital occupancies and their parent and atomic charges, atomic hybrid contribution to atomic bonds and the delocalisation of electron density, within the molecule.

In Table 7, the natural atomic orbitals, their occupancies and the corresponding energy of TD were described. In a given molecular environment the natural atomic orbitals reflect the chemical give and take of electronic interactions, with variations of shape (e.g., angular deformations due to steric pressures of adjacent atoms) and size (e.g., altered diffuseness due to increased anionic and cationic character) that distinguish them appreciably from free atom forms. The natural atomic orbital (NAO) energies $\varepsilon_i^{(A)}$ are calculated by using Kohu-sham operator (F) as

$$\varepsilon_i^{(A)} = \langle \theta_i^{(A)} | F | \theta_i^{(A)*} \rangle$$

The NAOs deals the molecular properties in terms of inter atomic and intra-atomic contributions. Table 8 depicts the bonding concepts such as type of bond orbital, their occupancies, the natural atomic hybrids of which the NBO is composed, giving the percentage of the NBO each hybrid, the atom label and a hybrid label showing the hybrid orbital composition (the amount of S-character, p-character, etc.,) of TD molecule determined by B3LYP/6-311++G(d,p) method with respectable accuracy. The occupancies of NBOs in TD reflecting their exquisite dependence on the chemical environment. The NBO energy values show the corresponding spatial symmetry breaking in the direction of unpaired spin. The Lewis structure that is closest to the optimised structure is determined the hybridisation of the atoms and the weight of each atom in each localised electron pair bond is calculated in this idealised Lewis structure and presented in Table 8.

For example, the bonding orbital for N_1-N_2 with 1.98845 electrons has 46.48% N_1 character in a $sp^{2.44}$ hybrid and has 53.52% N_2 character in a $sp^{2.07}$ hybrid orbital of TD. The bonding orbital C_3-O_8 with 1.98706 electrons has 41.45% C_3 character in a $sp^{2.16}$ hybrid and has 58.55% O_8 character in a $sp^{3.89}$ hybrid orbital. A bonding orbital for N_4-H_9 with 1.97964 electrons has 73.29% N_4 character in $sp^{2.43}$ hybrid and has 26.71% H_9 character in a s orbital. The C_5-C_6 with 1.98632 electrons has 50.11% C_5 character in a $sp^{1.58}$ hybrid and has 49.89% C_6 character in a $sp^{1.80}$ hybridised orbital.

8.1 Donor acceptor interactions: Perturbation theory energy analysis

The localised orbitals in the Lewis structure of TD can interact strongly. A filled bonding or lone pair orbital can act as a donor and an empty or filled bonding, anti-bonding, or lone pair orbital can act as an acceptor. These interactions can strengthen and weaken bonds. For example, a lone pair donor

Table 8.Bond orbital analysis of 1,2,4-triazine-3,5(2H,4H)-dione by B3LYP/6-311++G(d,p).

Bond Orbital	Occupancy	Atom	Contribution from parent NBO (%)	Atomic hybrid Contributions (%)
N1-N2	1.98845	N1	46.48	s(28.99) + p(70.88)
		N2	53.52	s(32.53) + p(67.39)
N1-C6	1.98477	N1	59.99	s(39.53) + p(60.38)
		C6	40.01	s(21.91) + p(69.98)
N1-C6	1.83406	N1	53.29	s(0.00) + p(99.83)
		C6	46.71	s(0.00) + p(99.82)
N2-C3	1.99133	N2	63.35	s(36.63) + p(63.31)
		C3	37.65	s(33.78) + p(66.10)
N2-H7	1.98318	N2	72.34	s(30.85) + p(69.11)
		H7	27.66	s(99.94) + p(0.06)
C3-N4	1.98456	C3	37.24	s(34.44) + p(65.45)
		N4	62.76	s(34.50) + p(65.4.3)
C3-O8	1.98706	C3	41.45	s(31.63) + p(68.26)
		O8	58.55	s(20.41) + p(79.50)
C3-O8	1.98476	C3	25.13	s(0.00) + p(99.74)
		O8	74.87	s(0.00) + p(99.94)
N4-C5	1.98598	N4	63.36	s(36.28) + p(63.67)
		C5	36.64	s(31.18) + p(68.70)
N4-H9	1.97964	N4	73.29	s(29.12) + p(70.85)
		H9	26.71	s(99.94) + p(0.06)
C5-C6	1.98632	C5	50.11	s(38.73) + p(61.20)
		C6	49.89	s(35.71) + p(64.22)
C5-O10	1.98841	C5	40.61	s(29.87) + p(70.02)
		O10	59.39	s(21.63) + p(78.28)
C5-O10	1.95412	C5	28.03	s(0.00) + p(99.81)
		O10	71.97	s(0.00) + p(99.94)
C6-H11	1.97721	C6	62.14	s(34.48) + p(65.48)
		H11	37.86	s(99.95) + p(0.05)

→ anti-bonding acceptor orbital interaction may weaken the bond associated with the anti-bonding orbital. Conversely, an interaction with a bonding pair as the acceptor may strengthen the bond. Strong electron delocalisation in the Lewis structure also shows up as donor–acceptor interactions. The important bonding and anti-bonding orbitals of the bonds of TD are presented below:

- π (N_1-N_2) = 0.6818 ($sp^{2.44}$)N_1 + 0.7316 ($sp^{2.07}$)N_2
- π^*(N_1-N_2) = 0.7316 ($sp^{2.44}$)N_1 - 0.6818 ($sp^{2.07}$)N_2
- π (N_1=C_6) = 0.7745 ($sp^{1.53}$)N_1 + 0.6325 ($sp^{2.34}$)C_6
- π^*(N_1=C_6) = 0.6325 ($sp^{1.53}$)N_1 – 0.7745 ($sp^{2.34}$)C_6
- σ (N_1=C_6) = 0.7300 ($sp^{1.00}$)N_1 + 0.6835 ($sp^{1.00}$)C_6
- σ^*(N_1=C_6) = 0.6835($sp^{1.00}$)N_1 - 0.7300 ($sp^{1.00}$)C_6
- π (N_2=C_3) = 0.7896($sp^{1.73}$)N_2 + 0.6136 ($sp^{1.96}$)C_3
- π^*(N_2-C_3) = 0.6136($sp^{1.73}$)N_2 - 0.7896 ($sp^{1.96}$)C_3
- π (C_3-N_4) = 0.6102($sp^{1.90}$)C_3 + 0.7922($sp^{1.90}$)N_4
- π^*(C_3-N_4) = 0.7922($sp^{1.90}$)C_3 - 0.6102($sp^{1.90}$)N_4
- π (N_4-C_5) = 0.7960($sp^{1.75}$)N_4 + 0.6053($sp^{2.20}$)C_5
- π^*(N_4-C_5) = 0.6053($sp^{1.75}$)N_4 - 0.7960($sp^{2.20}$)C_5
- π (C_5-C_6) = 0.7079($sp^{1.58}$)C_5 + 0.7063($sp^{1.80}$)C_6
- π^*(C_5-C_6) = 0.7063($sp^{1.58}$)C_5 - 0.7079($sp^{1.80}$)C_6

The electrostatic potential of bonding molecular orbital of C=O, anti-bonding molecular orbital of C=O, bonding molecular orbital of C_6=N_1 and anti-bonding molecular orbital of C_6=N_1 of TD.

The stabilisation energy of different kinds of interactions are listed Table 9. This calculation is done by examining all possible interactions between 'filled' (donor) Lewis-type NBOs and 'empty' (acceptor) non-Lewis NBOs, and estimating their energetic importance by second-order perturbation theory. Since these interactions lead to loss of occupancy from the localised NBOs of the idealised Lewis structure into the empty non-Lewis orbitals (and thus, to departures from the idealised Lewis structure description), they are referred to as 'delocalisation' corrections to the natural Lewis structure. The NBO method demonstrates the bonding concepts like atomic charge, Lewis structure, bond type, hybridisation, bond order, charge transfer and resonance weights. Natural bond orbital analysis is a useful tool for understanding delocalisation of electron density from occupied Lewis-type (donor) NBOs to properly unoccupied non-Lewis type (acceptor) NBOs within the molecule. The stabilisation of orbital interaction is proportional to the energy difference between interacting orbitals. Therefore, the interaction having strongest stabilisation takes place between effective donors and effective acceptors. This bonding-anti bonding interaction can be quantitatively described in terms of the NBO approach that is expressed by means of second-order perturbation interaction energy $E^{(2)}$ [78–81]. This energy represents the estimate of the off-diagonal NBO Fock matrix element. The stabilisation energy $E^{(2)}$ associated with i (donor)→j (acceptor) delocalisation is estimated from the second-order perturbation approach as [82] given below

$$E^{(2)} = q_i \frac{F^2(i,j)}{\varepsilon_j - \varepsilon_i}$$

where, q_i is the donor orbital occupancy, ε_i and ε_j are diagonal elements (orbital energies) and F^2(i, j) is the off-diagonal Fock matrix element.

9. Analysis of molecular electrostatic potential (MESP)

Molecular electrostatic potential (MESP) useful quantities to illustrate the charge distributions of molecules are used to visualize variably charged regions of a molecule. Therefore, the charge distributions can give the information about how the molecules interact with another molecule. At any given point r(x, y, z) in the vicinity of a molecule, the MESP, V(r) is defined in terms of the interaction energy between the

Table 9.Second order perturbation theory analysis of Fock matrix of 1,2,4-triazine-3,5(2H,4H)-dione by NBO method.

Donor (i)→Acceptor (j)	$E^{(2)a}$ (kJ mol^{-1})	E(j) - E(i)[b] (a.u)	F(I, j)[c] (a.u)
π(N1-N2) → π*(N2-C3)	1.26	1.44	0.038
π(N1-N2) → π*(C3-O8)	2.29	1.30	0.049
π(N1-N2) → π*(C6-H11)	0.94	1.43	0.033
π(N1-C6) → π*(N2-H7)	2.73	1.25	0.052
π(N1-C6) → π*(C5-C6)	0.68	1.40	0.028
π(N1-C6) → π*(C5-O10)	2.73	1.19	0.051
σ(N1-C6) → σ*(N1-C6)	3.77	0.31	0.031
σ(N1-C6) → σ*(C5-O10)	23.75	0.29	0.079
π(N2-C3) → π*(N1-N2)	0.97	1.37	0.033
π(N2-C3) → π*(N2-H7)	0.61	1.28	0.025
π(N2-C3) → π*(N4-H9)	1.70	1.29	0.042
π(N2-H7) → π*(N1-C6)	4.45	1.22	0.066
π(N2-H7) → π*(N2-C3)	0.63	1.16	0.024
π(N2-H7) → π*(C3-N4)	3.87	1.18	0.061
π(C3-N4) → π*(N2-H7)	1.47	1.27	0.039
π(C3-N4) → π*(N4-C5)	2.27	1.39	0.050
π(C3-N4) → π*(N4-H9)	0.76	1.29	0.028
π(C3-N4) → π*(C5-O10)	3.46	1.22	0.058
π(C3-O8) → π*(N1-N2)	2.78	1.22	0.052
π(C3-O8) → π*(N4-C5)	2.37	1.24	0.049
σ(C3-O8) → σ*(C3-O8)	4.38	0.24	0.033
π(N4-C5) → π*(C3-N4)	1.99	1.35	0.047
π(N4-C5) → π*(C3-O8)	3.05	1.20	0.054
π(N4-C5) → π*(N4-H9)	1.10	1.29	0.034
π(N4-C5) → π*(C5-C6)	0.76	1.42	0.029
π(N4-C5) → π*(C6-H11)	0.96	1.33	0.032
π(N4-H9) → π*(N2-C3)	4.13	1.15	0.062
π(N4-H9) → π*(C3-N4)	0.93	1.16	0.030
π(N4-H9) → π*(C3-O8)	0.63	1.01	0.023
π(N4-H9) → π*(N4-C5)	1.02	1.19	0.031
π(N4-H9) → π*(C5-C6)	3.01	1.23	0.054
π(N4-H9) → π*(C5-O10)	0.65	1.02	0.023
π(C5-C6) → π*(N1-C6)	0.61	1.25	0.025
π(C5-C6) → π*(N4-C5)	0.79	1.24	0.028
π(C5-C6) → π*(N4-H9)	3.24	1.14	0.054
π(C5-C6) → π*(C6-H11)	1.02	1.19	0.031
π(C5-O10) → π*(N1-C6)	1.90	1.25	0.043
π(C5-O10) → π*(C3-N4)	2.32	1.21	0.048
π(C5-O10) → π*(C5-C6)	0.70	1.27	0.048
σ(C5-O10) → σ*(N1-C6)	10.91	0.27	0.051
σ(C5-O10) → σ*(C5-O10)	1.61	0.25	0.020
π(C6-H11) → π*(N1-N2)	5.08	1.02	0.064
π(C6-H11) → π*(N1-C6)	0.68	1.05	0.024
π(C6-H11) → π*(N4-C5)	4.12	1.04	0.059
π(C6-H11) → π*(C5-C6)	0.87	1.07	0.027

[a]Stabilisation (delocalisation) energy

[b]Energy difference between I (donor) and j(acceptor) NBO orbitals.

[c]Fock matrix element I and j NBO orbitals.

electrical charge generated from the molecule electrons and nuclei and a positive test charge (a proton) located at [83,84].

$V(r) = \Sigma Z_A / |R_A - r| - \int \rho(r') / |r' - r| \, dr'$

Where the summation runs over all the nuclei A in the molecule and polarization and reorganization effects is neglected. Z_A is the charge of the nucleus A, located at R_A and $\rho(r')$ is the electron density function of the molecule. The total electron density and MESP surfaces of the molecules under investigation are constructed by using B3LYP/6-311++G(d,p) method. The total electron density surface of TD are shown in Fig. 7 while the total electron density surface

mapped with the electrostatic potential of TD are shown in Fig. 8. The electrostatic potential contour maps for positive and negative potentials are shown in Fig. 9. The colour scheme for the MESP surface is red, electron rich, partially negative charge; blue, electron deficient, partially positive charge; light blue, slightly electron deficient region; yellow, slightly electron rich region; green, neutral; respectively. The electrostatic potential surface of the title compound are presented in Fig. 10.

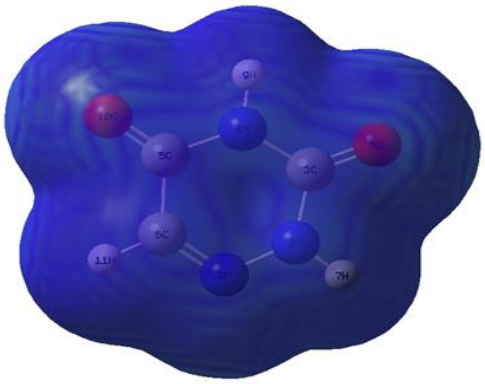

Fig 7.The total electron density surface of 1,2,4-triazine3,5(2H,4H)dione.

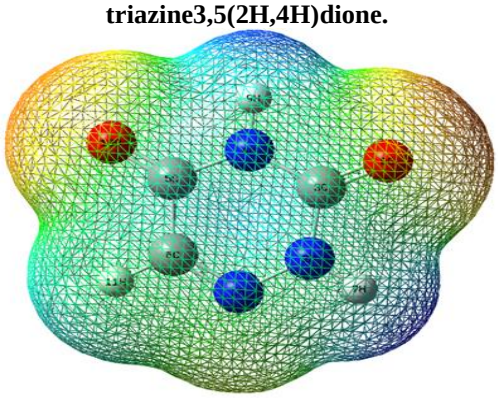

Fig 7a.DFT (B3LYP)/6-311+G(d,p) calculated 3D total electron density mapped surface of 1,2,4-triazine-3,5(2H,4H)-dione.

The molecular electrostatic potential is related to the electronic density and a very useful descriptor for determining sites for electrophilic attack and nucleophile reactions as well as hydrogen-bonding interactions [85–87]. In Fig.7, whereas electrophilic reactivity was presented by negative (red) regions, oxygen reactivity was shown by the positive (blue) regions of MEP. As seen from figure, the red region was localized on the vicinity of nitro an oxygen groups for all the compounds studied in this work DFT (B3LYP)/6-311++G(d,p) total electron density mapped surface of TD in Fig 7(a). These regions reflect the most electronegative region (excess negative charge). It is visible that there is more electronegative region in TD compound. On the other hand, the nitrogen and oxygen reactivity of the molecules was localized on the hydrogen atoms. In this respect, the TD was found to be useful to both bonds metallically and interact intermolecular. Based on these results, it can be ascertained that how the change of the fluorine group affects the molecular properties of the title compounds. Moreover, according to the ESP figures, the most negative ESP is spread over the oxygen and fluorine atoms, indicating the delocalization of π-electrons over nitro an oxygen groups for all the molecules (Fig. 9). This also reveals extended conjugation of the benzene ring with these groups. Furthermore, the total charge density contour is given in the same figure. One can see from Fig. 8(a) blue color in TD is found to be the predominance because of the positive charge distribution of the molecule.

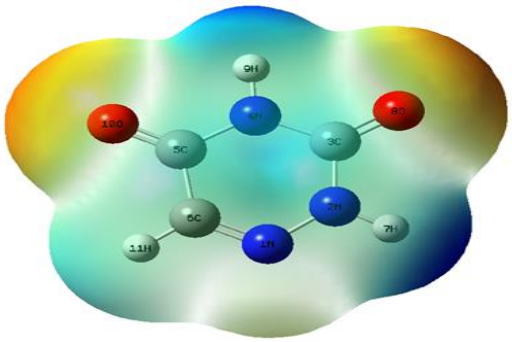

Fig 8. Total electron density surface mapped with electrostatic potential of 1,2,4- triazine-3,5(2H,4H)-dione.

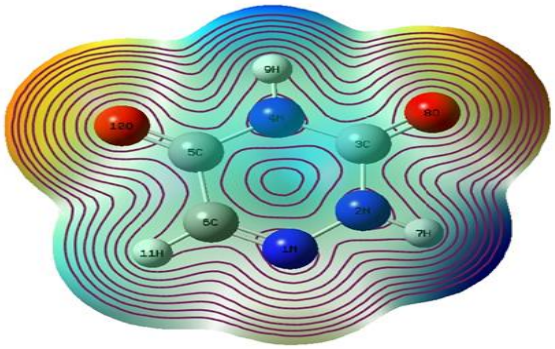

Fig 8a. Total electron density surface contour mappedwith electrostatic potential of 1,2,4-triazine-3,5(2H,4H)-dione.

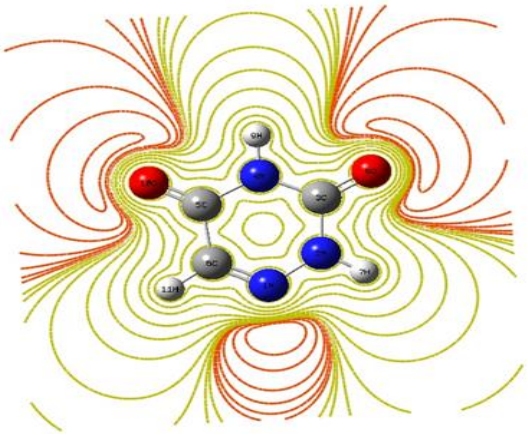

Fig 9. Contour map of electrostatic potential 1,2,4-triazine-3,5(2H,4H)-dione.

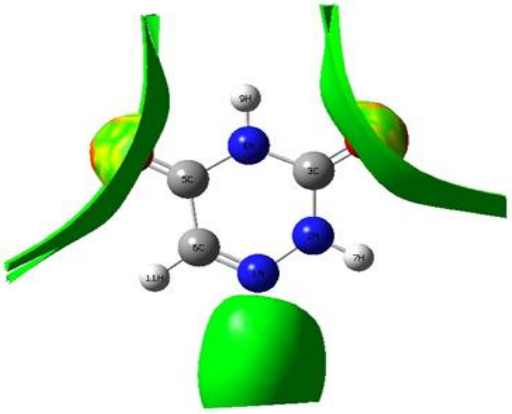

Fig 10 . Electrostatic potential surface of 1,2,4-triazine-3,5(2H,4H)-dione.

10. Conclusion

The vibrational properties of TD have been investigated by FT-IR and FT-Raman spectroscopies and were performed on the basis of *ab initio* HF and DFT/B3LYP method with 6-311++G(d,p) basis set level. Attempts have been made in the present work for the proper frequency assignment of the title compound. The influence of C-H, N-H, C=O and C-N in the vibrational frequencies of TD were discussed. The theoretical results were compared with the observed vibrational wave numbers. The deviation between the experimental and calculated frequencies were reduced with the use of DFT/B3LYP/6-311++G(d,p) basis sets. The HOMO-LUMO energy gap of TD were calculated at DFT/B3LYP/6-311++G(d,p) level revels that the energy gap reflect the chemical activity of the molecule. Lower in the HOMO and LUMO energy gap supports bioactive property of the molecule. NBO analysis has also been performed on TD molecule, in order to elucidate intermolecular hydrogen bonding, intermolecular charge transfer, rehybridization and delocalization of electron density. The MESP map shows that the negative potential sites are on oxygen atoms as well as positive potential sites on around hydrogen atoms. These may provide information about the possible reaction regions for the title compound.

References

[1] P. Vicini, M.I. Incerti, P.L. Colla, R. Loddo, Eur. J. Med. Chem. 44(2009)1801–1807.
[2] S.K. Bharti, G. Nath, R. Tilak, S.K. Singh,. Eur. J. Med. Chem. 45(2010) 651–660.
[3] P. Vicini, F. Zani, P.Cozzini, I. Doytchinova, Eur. J. Med. Chem. 37(2002) 553–567.
[4] F.D. Popp, Eur. J. Med. Chem. 24(1989) 313–316.
[5] S.K. Sridhar, S.N. Pandeya, J.P. Stables, R. Atmakuru, Eur. J. Pharm. Sci. 16(2002) 129–132.
[6] A.R. Todeschini, A.L.P. Miranda, K.C.M. Silva, S.C. Parrini, E. Barreiro, Eur. J. Med. Chem. 33(1998)189–199.
[7] P. Melnyk, V. Leroux, C. Sergheraert, P. Grellier, Bioorg. Med. Chem. Lett. 16(2006)31–35.
[8] Y.A. Ibrahim, Carbohyd. Lett. 1(1996) 425-432.
[9] Y.A. Ibrahim, Carbohyd. Lett. 2(1996) 189-195.
[10] A.K. Mansour, Y.A. Ibrahim, N.A.S.M. Khalil, Nucleos. Nucleot.18(1999) 2265- 2283.
[11] Z.X. Kang, Y. Li , K. Mori, Mater. Sci. Forum., 488 (2005) 661-672.
[12] Z.X. Kang, J. Sang, M. Shao, Y. Li, J. Mater. Process. Tech., 209 (2009) 4590-4598.
[13] D.P. Roy, Bioorg. Med. Chem (1970) 42-45.
[14] R.K. Robins, Chem. Eng. News 64(1986) 28-40.
[15] C. Bonini, L. Chiummiento, M.D. Bonis, M. Funicello, P. Lupattelli, G. Suanno, F.
Berti, P. Campaner, Synthesis Tetrahedron 61(2005) 6580-6589.
[16] L. Brault, E. Migianu, A. Neguesque, E. Battaglia, D. Bagrel, G. Kirsch, Eur. J. Med.
Chem .40(2005)757-763.
[17]P.R. Kumar, S. Raju, P.S. Goud, M. Sailaja, M.R. Sarma, G.O. Reddy, M.P. Kumar,
V.V.R.M.K. Reddy, T. Suresha, P. Hegdeb, Bioorg. Med. Chem.12(2004) 1221-1230.
[18] J. Graff, S. Harder, O. Wahl, E.H. Scheuermann, J. Gossmann, Clin. Pharmacol. Ther.78 (2005)468-476.
[19]A. Hymete, J. Rohloff, H. Kjosen, T.H. Iversen, Ethiopia. Nat. Prod. Res.19(2005) 755-761.
[20] R.A. Tapia, L. Alegria, C.D. Pessoa, C. Salas, M.J. Cortes, J.A. Valderrama, M.E. Sarciron, F. Pautet, N. Walchshofer, H. Fillion, Bioorg. Med. Chem. 11(2003)2175-2182.
[21] P. Dallemagne, L.P. Khanh, A. Alsaidi, I. Varlet, V. Collot, M. Paillet, R. Bureau, S. Rault, Bioorg. Chem. 11(2003)1161-1167.
[22] M.P. Kumar, G. Panda, Y.K. Manju, V. Chaturvedi, S. Sinha, Bioorg. Med. Chem. Lett. 18(2008)289-292.
[23] R.M. Abdel-Rahman, Part II. Pharmazie. 166(2000)315-357.
[24] R.M. Abdel-Rahman, Part III. Pharmazie. 54(1999)791-803.
[25] H.A. Saad, H.A. Allimony, F.A.A. El-Mariah, Part 2. Indian J. Chem. 37B(1998) 1142-1148.
[26] F.A.A. El-Mariah, H.A. Saad, H.A. Allimony, R.M. Abdel-Rahman, Part 3. Indian J. Chem. 39B(2000)36-41.
[27] J. Salimon, N. Salih, Int. J. PharmTech Res. 2(2010)1041-1045.
[28] J.N. Sangshetti, D.B. Shinde, Med. Chem. Lett. 20(2010)742-745.
[29] R.M. Abdel-Rahman, A Review. Pharmazie 56(2001)18-22.
[30] Z. El-Gendy, J.M. Morsy, H.A. Allimony, W.R. Abdel-Monem, R.M. Abdel-
Rahman, Part III. Pharmazie 56(2001)376-383.
[31] C. Gill, G. Jadhav, M. Shaikh, R. Kale, A. Ghawalkar, D. Nagargoje, M. Shiradkar, Med. Chem. Lett. 18(2008)6244-6247.
[32] P. Mullick, S.A. Khan, T. Begum, S. Verma, D. Kaushik, O. Alam, Acta Pol. Pharm. Drug Res. 66(2009)379-385.
[33] J. Hynes, S.B. Kanner, X. Yang, J.S. Tokarski, G.L. Schieven, A.J. Dyckman, H.
Lonial, R. Zhang, J.S. Sack, S. Lin, J. Med. Chem. 51(2008)4-16.
[34] R.M. Abdel-Rahman, A Review. Pharmazie 56(2001)195-204.
[35] R.M. Abdel-Rahman, Z. El-Gendy, M.B. Mahmoud, Indian J.Chem. 29B(1990)352-358.
[36] R.M. Abdel-Rahman, M.S. Abdel-Malik, Pak. J. Sci. Ind. Res. 33(1990)142-147.
[37] R.M. Abdel-Rahman, M. Seada, Z. El-Gendy, I.E. Islam, M.B. Mahmoud, Farmaco
48(1993)407-416.
[38] Hiroyuki Isobe et al. Org. Lett.10(2008) 3729–3732.
[39] M.B. Klix, J.A. Verreet, M. Beyer, Crop. Prot. 26(2007)683-690.
[40] U. Gisi, H. Sierotzki, A. Cook, A. McCaffery, Pes. Mana. Sci. 58(2002)859–867.
[41] H.J. Frisch, G.W. Trucks, H.B. Schlegel, G.E. Scuseria, M.A. Robb, J.R. Cheeseman,
H. Nakatsuji, M. Caricato, X. Li, H.P. Hratchian, K. Toyota, R. Fukuda, J. Hasegawa,
M. Ishida, R. Nakajima, Y. Honda, O. Kilao, H. Nakai, T. Verven, J. A. Montgomery
Jr., J.E. Peralta, F. Ogliaro, M. Bearpark, J. J. Heyd, E. Brothers, K. N. Kudin,
V.N. Staroverov, R. Kobayashi, J. Normand, K. Ragavachari, A. Rendell, J.C.
Burant, S. J. Tomasi, M. Cossi, N. Rega, J. M. Millam, M. Klene, J. E. Knox, J. B.
Cross, V. Bakken, C. Adamo, J. Jaramillo, R. Gomperts, R.E. Strattmann, O. Yazyev,

A.J. Austin, R. Cammi, J.W. Ochetrski, R.L. Martin, K. Morokuma, V.G. Zakrazawski, G.A.Votn, P. Salvador, J.J. Dannenberg, S. Dapprich, A.D. Daniels, O. Farkas, J.B. Foresman, Gaussian O.G., Revision A.O2, Gaussian Inc., Wallingford, CT. 2009.
[42] A.D. Becke, J. Chem. Phys. 98 (1993) 5648 – 5652.
[43] C. Lee, W. Yang, R.G. Parr, Phys. Rev. B37 (1998) 785 – 789.
[44] G. Rahut, R. Pulay, J. Phys. Chem. 99 (1995) 3093 – 3100.
[45] R. Pulay, G. Fogarasi, G. Pongor, J.E. Boggs, A. Vargha, J. Am. Chem. Soc. (1983) 7037 – 7047.
[46] G. Fogarassi, P. Pulay, in: J. R. Durig (Ed.), Vibrational Spectra and Structure, Vol.14, Elsevier, Amsterdam, 1985, P 125 (Chapter 3)
[47] G. Fogarassi, X. Zhou, P.W. Taylor, P. Pulay, J. Am. Chem. Soc. 114 (1992) 8191 – 8201.
[48] T. Sundius, J. Mol. Struct., 218 (1990) 321 – 326.
[49] T. Sundius, Vib. Spectrosc., 29 (2002) 89 – 95
[50] MOLVIB (V.7.0): Calculation of Harmonic Force Fields and Vibrational Modes of Molecules, QCPE Program No. 807 (2002).
[51] H.F. Hameka, J.O. Jensen, J. Mol. Struct. (Theochem.) 362 (1996) 325.
[52] J.O. Jensen, A. Banerjee, C.N. Merrow, D. Zeroka, J.M. Lochner, J. Mol. Struct.
(Theochem.) 531 (2000) 323-332.
[53] A.P. Scott, L. Radom, J. Phys. Chem. 100 (1996) 1652-1664.
[54] M.P. Andersson, P. Uvdal, J. Chem. Phys. A109 (2005) 2937-2946.
[55] M. AlcoleaPalafox, M. Gill, N.J. Nunez, V.K. Rastogi, Lalit Mittal, Rekha Sharma, Int. J. Quant. Chem. 103 (2005) 394-412.
[56] M. AlcoleaPalafox, Int. J. Quant. Chem. 77 (2000) 661-672.
[57] V. Arjunan, P. Ravindran, T. Rani, S. Mohan, J. Mol. Struct. 988 (2011) 91-104.
[58] P.L. Polavarappu, J. Phys. Chem. 94 (1990) 8106–8112.
[59] G. Keresztury, S. Holly, J. Varga, G. Besenyei, A.Y. Wang, J.R. Durig, Spectrochim.
Acta A 49 (1993) 2007–2202.
[60] V. Krishnakumar, G. Keresztury, T. Sundius, R. Ramasamy, J. Mol. Struct. 702 (2004) 9-18.
[61] P. Pulay, G. Fogarasi, F. Pang, J.E. Boggs, J. Am. Chem. Soc. 101 (1979) 2550-2563.
[62] G. Fogarasi, X. Zhou, P.W. Taylor, P. Pulay, J. Am. Chem. Soc. 114 (1992) 819– 821.
[63] Varsanyi, Assignment for vibrational Spectra of Seven Hundred Benzene Derivatives, Vol. 1–2, Academic Kiaclo, Budapest, 1973.
[64] M. Silverstein, G. Clayton Basseler, C. Morill, Spectrometric Identification of Organic Compounds, Wiley, New York, 1981.
[65] C.P. D. Dwivedi, S.N. Sharma, Indian J. Pure Appl. Phys. 11 (1973) 447-456.
[66] D. Becke, J. Chem. Phys. 98 (1993) 5648–5652.
[67] F.S. Mortimer, R.B. Blodgett, F. Daniels, J. Am. Chem. Soc. 69 (1947) 822-834.
[68] N. Puviarasan, V. Arjunan, S. Mohan, Turk. J. Chem. 26 (2002) 323-334.
[69] V. Arjunan, P.S. Balamourougane, S.T. Govindaraja, S. Mohan, J. Mol.Struet 1018(2012)156-170.
[70] V.Krishanakumar, N. Prabavathi, Spectrochim Acta A77(2010) 238-247.
[71] M.T. Gulluoglu, M. Ozduran, M. Kurt, S. Kalaichelvan, N. Sundaraganesan, Spectrochim.Acta, A 76(2010)107-114.
[72] D.N. Sathyanarayana, Vibrational Spectroscopy, Theory and Applications, New Age International Publishers, New Delhi, 2004.
[73]R.L. Prasad, A. Kushwaha, M. Suchita, R.A. Jumar, Spectrochim. Acta. A69(2008)304-311.
[74]M. Amalanethan, V.K. Rastogi, I. Hubert Joe, M.A. Palatox, R.Tomar, Spectrochim. Acta A 78(2011) 1437- 1444.
[75]R.J. Xavier, E. Gopinath, Spectrochim Acta Part A 91(2012) 248-255.
[76] Y. Atalay, D. Avii, A. Basaoglu, Struct. Chem. 19 (2008) 239-252.
[77]T. Vijayakumar, I. Hubertjoe, C.P.R. Nair, V.S. Jayakumar, Chem. Phys. 343 (2008) 83–89.
[78] A.E. Reed, F. Weinhold, J. Chem. Phys. 83 (1985) 1736-1747.
[79] A.E. Reed, R.B. Weinstock, F. Weinhold, J. Chem. Phys. 83 (1985) 735-743.
[80] A.E. Reed, F. Weinhold, J. Chem. Phys. 78 (1983) 4066-4072.
[81] J.P. Foster, F. Weinhold, J. Am. Chem. Soc. 102 (1980) 7211-7219.
[82] J.M. Seminario, Recent Developments and Applications of Modern Density Functional Theory, Vol. 4, Elsevier, Amsterdam, 1996. pp. 800–806.
[83]N. Ozdemir, B. Eren, M. Dincer, Y. Bekdemir, Mol. Phys. 108 (2010) 13–24.
[84] P. Politzer, J.S. Murray, Theor. Chem. Acc. 108 (2002) 134–142.
[85]F.J. Luque, J.M. Lopez, M. Orozco, Theor. Chem. Acc. 103 (2000) 343–345.
[86] N. Okulik, A.H. Jubert, Internet Electron, J. Mol. Des. 4 (2005) 17–30.
[87]C. Parlak, M. Akdogan, G. Yildirim, N. Karagoz, E. Budak, C. Terzioglu, Spectrochim. Acta A 79 (2011) 263–271.